

# On Relativistic Corrections to Microlensing Effects: Applications to the Galactic Black Hole

A. O. Petters

*Duke University, Department of Mathematics, Durham, NC 27708, USA*

2002, July 31

## ABSTRACT

The standard treatment of gravitational lensing by a point mass lens  $M$  is based on a weak-field deflection angle  $\hat{\alpha} = 2/x_0$ , where  $x_0 = r_0 c^2 / 2GM$  with  $r_0$  the distance of closest approach to the mass of a lensed light ray. It was shown that for a point mass lens, the total magnification and image centroid shift of a point source remain unchanged by relativistic corrections of second order in  $1/x_0$ . This paper considers these issues analytically taking into account the relativistic images, under three assumptions **A1–A3**, for a Schwarzschild black hole lens with background point and extended sources having arbitrary surface brightness profiles. The assumptions are **A1**: The source is close to the line of sight and lies in the asymptotically flat region outside the black hole lens; **A2**: The observer-lens and lens-source distances are significantly greater than the impact parameters of the lensed light rays; and **A3**: The distance of closest approach of any light ray that does not wind around the black hole on its travel from the source to the observer, lies in the weak-field regime outside the black hole. We apply our results to the Galactic black hole for lensing scenarios where **A1–A3** hold. We show that a single factor characterizes the full relativistic correction to the weak-field image centroid and magnification. As the lens-source distance increases, the relativistic correction factor strictly decreases. In particular, we find that for point and extended sources about 10 pc behind the black hole, which is a distance significantly outside the tidal disruption radius of a sun-like source, the relativistic correction factor is minuscule, of order  $10^{-14}$ . Therefore, for standard lensing configurations, any detectable relativistic corrections to microlensing by the Galactic black hole will most likely have to come from sources significantly closer to the black hole.

**Key words:** black holes: strong field regime – gravitational lensing: photometry and astrometry.

## 1 INTRODUCTION

Microlensing describes gravitational lensing of a source whose multiple images are not resolved. Two fundamental microlensing observables are the total magnification (photometry) and image centroid shift (astrometry) of images of a lensed source. These observables have important astrophysical applications such as determining the mass and distance to the lens, angular radius of the source, etc. (see, e.g., Paczynski 1996, Paczyński 1998, Boden, Shao & van Buren 1998, Jeong, Han & Park 1999, Gaudi & Petters 2002, and references therein).

A natural issue to explore is how are the photometry and astrometry of a source being lensed by a point mass changed when the point mass is replaced by a black hole

lens. This could have important implications for the testability of general relativity’s predictions about how the gravitational field of a black hole affects light rays. Indeed, the standard theoretical framework for point mass microlensing is based on relativistic calculations to first-order in  $1/x_0$  about a Schwarzschild black hole, where

$$x_0 = \frac{r_0}{2r_g}, \quad r_g = \frac{GM_\bullet}{c^2},$$

where  $M_\bullet$  is the black hole’s mass and  $r_g$  the gravitational radius. Ebina et al. (2000) found that to second-order in  $1/x_0$ , the relativistic corrections appear in the position and magnification of images due to a point mass lens, while no such correction appears in the total magnification. Lewis & Wang (2001) also showed that no relativistic correction

arXiv:astro-ph/0208500v2 16 Sep 2002

to second-order in  $1/x_0$  occurs for the associated image centroid shift. In this paper, we extend the work of the previous authors by determining an analytical expression under assumptions **A1–A3** for the full Schwarzschild black hole relativistic correction of the image centroid shift, which includes the total magnification, for point and extended sources with arbitrary surface brightness.

The full relativistic corrections will then be applied to the case of the massive black hole at the center of our Galaxy. Microlensing by the Galactic black hole has been studied by several authors in the weak-field limit of the black hole (e.g., Wardle & Yusef-Zadeh 1992, Alexander & Sternberg 1999, Alexander & Loeb 2001, Alexander 2001). In addition, the precession of star orbits in the strong-field regime of the black hole was considered by, e.g., Jaroszynski (1998a,b, 1999), Fragile & Mathews (2000). Virbhadra & Ellis (2000) gave a numerical treatment of the magnifications of several relativistic images for a point source being lensed by a Schwarzschild black hole lens at the Galactic center. They considered sources within our Galaxy that are far away from the black hole (about 8.5 kpc), while we shall consider sources as close as 10 pc to the black hole. Analytical work on magnification due to a Schwarzschild lens was also done by several authors for point and/or extended sources with uniform brightness profiles (e.g., Ohanian 1987, Frittelli, Kling & Newman 2000, Bozza et al. 2001, Eiroa, Romero & Torres 2002). As noted above, our microlensing treatment will apply not only to the magnification, but the image centroid of extended sources with arbitrary surface brightness.

We shall also show that a single factor approximates the relativistic corrections to the weak-field total magnification and image centroid due to a Schwarzschild black hole lens at the Galactic center. The same factor applies to either a point or extended source. Estimates of this factor will be given for lens-sources distances ranging from 10 pc to 100 pc. In principle, the magnification and image centroid of sources closer to the Galactic black hole should provide stronger relativistic microlensing signatures. We shall show that even for sources about 10 pc behind the black hole, the full relativistic correction is still negligible.

Section 2 reviews some basic results about lensing by a Schwarzschild black hole. In Section 3, we compute explicitly the image centroid due to a Schwarzschild black hole acting on point and extended sources with arbitrary brightness profiles. Our image centroid formula expresses the relativistic image centroid in terms of the weak-field image centroid due to a point mass lens. Section 4 estimates the relativistic corrections to microlensing by the Galactic black hole.

## 2 IMAGE POSITION AND MAGNIFICATION

We review some basic analytical results about the image positions and magnification due to a Schwarzschild black hole lens.

### 2.1 Lens Equation and Bending Angle

A Schwarzschild black hole of mass  $M_\bullet$  is the unique static, spherically symmetric, vacuum (i.e., Ricci flat) spacetime

that is Minkowski at infinity (e.g., Wald 1984, p. 119):

$$ds^2 = - \left(1 - \frac{r_\bullet}{r}\right) c^2 dt^2 + \left(1 - \frac{r_\bullet}{r}\right)^{-1} dr^2 + r^2 d\Omega^2$$

where  $r_\bullet$  is the Schwarzschild radius

$$r_\bullet = 2r_g = 3 \frac{M_\bullet}{M_\odot} \text{ km}$$

and  $d\Omega^2$  the standard metric on a 2-sphere of radius 1.

Relative to the optical axis through the observer and center of the black hole, let  $\beta$  denote the angular position of a point source behind the black hole. Note that a source between the observer and the black hole is also lensed; in principle, even the observer is lensed. Such situations will not be treated in this paper. We shall always assume the standard lensing configuration of a source behind the black hole

The capture cross section  $\sigma$  of a light ray in a Schwarzschild spacetime is  $\sigma = \pi b_{\text{crit}}^2$ , where  $b_{\text{crit}} = 3\sqrt{3} r_g$  is the critical apparent impact parameter (e.g., Wald 1984, p.144). Consequently, any light ray that makes it from the source to the observer will have an apparent impact parameter  $b$  greater than  $b_{\text{crit}}$ . The classification of null geodesics in the Schwarzschild geometry divides such source-to-observer light rays into those that loop around the black hole at least once before arriving at the observer and those that travel directly to the observer without looping (cf. Misner, Thorne & Wheeler 1973, p. 674).

Let  $D_{LS}$ ,  $D_L$ , and  $D_S$  be the distances from lens to source, observer to lens, and observer to source, resp. Denote the angular position of a lensed image relative to the line of sight by  $\vartheta$ . A negative angle  $-\vartheta$  will correspond to an angular position on the side of the black hole opposite to the angular position  $\vartheta$ . A trigonometric argument yields the lens equation, which relates  $\beta$  and  $\vartheta$  as follows (Virbhadra & Ellis 2000):

$$\tan \beta = \tan \vartheta - \frac{D_{LS}}{D_S} (\tan \vartheta + \tan(\hat{\alpha} - \vartheta)), \quad (1)$$

where  $\hat{\alpha}$  is the bending angle of the lensed ray. The *lensed images* of a light source at  $\beta$  are the solutions  $\vartheta$  of the lens equation. The *magnification*  $\mu$  of a lensed image  $\vartheta$  is the ratio of the solid angle subtended at the distance to the source by the lensed image to the solid angle of the unlensed source. Explicitly,

$$\mu(\vartheta) = \left| \frac{\sin \beta(\vartheta)}{\sin \vartheta} \frac{d\beta}{d\vartheta}(\vartheta) \right|^{-1}. \quad (2)$$

The lens equation cannot be solved analytically in closed form, so approximations appropriate to the lensing scenario of interest to us will be employed.

Our working assumptions are:

**A1:** The source is assumed to be close to the line of sight, i.e.,  $|\beta| \ll 1$ , and lie in the asymptotically flat region outside the black hole, i.e.,  $D_{LS} \gg r_\bullet$ .

**A2:** In anticipation of later applications to the Galactic black hole, we suppose that  $D_L \gg b$  and  $D_{LS} \gg b$ , where  $b$  is the apparent impact parameter of *any* light ray from the source to the observer.

**A3:** For any light ray from the source to the observer that do not wind around the black hole, we shall assume that its

distance of closest approach  $r_0$  lies in the weak-field regime regime, i.e.,  $r_0 \gg r_\bullet$ .

We shall now use **A1** - **A3** to simplify the tangent terms in the lens equation. Relative to the observer, the caustic due to the black hole coincides with the optical axis passing the observer and singularity at  $r = 0$ . By **A1**, the source is near to the optical axis (i.e.,  $|\beta| \ll 1$ ), so the source is highly magnified and its angular position satisfies

$$\tan \beta \approx \beta. \quad (3)$$

In **A2**, it is important to add that the apparent impact parameter  $b$  and distance  $r_0$  of closest approach are not equal in general and approximate each other in the weak-field limit. In fact, for our lensing assumptions, the quantities  $b$  and  $r_0$  are related as follows (e.g., Wald (1984), p. 144)

$$b = \frac{r_0}{\sqrt{1 - r_\bullet/r_0}}.$$

Consequently, we have  $b > r_0$  and  $b \approx r_0$  for the nearly flat regime  $r_0 \gg r_\bullet$ . Assumption **A2** yields that  $|\tan \vartheta| \approx r_0/D_L \ll 1$ , so

$$\tan \vartheta \approx \vartheta. \quad (4)$$

Before discussing how our assumptions affect the term  $\tan(\hat{\alpha} - \vartheta)$  in (1), we consider the bending angle  $\hat{\alpha}$  under assumptions **A1** and **A2**. The bending angle, which is not a priori assumed to be small, is given by (e.g., Weinberg 1972, p. 189; Wald 1984, p. 145):

$$\hat{\alpha}(x_0) = 2 \int_{x_0}^{\infty} \frac{dx}{\sqrt{P(x)}} - \pi, \quad (5)$$

where

$$P(x) = x^2[(x/x_0)^2(1 - 1/x_0) - (1 - 1/x)], \quad x_0 = r_0/r_\bullet.$$

The integral in (5) is an elliptic integral and can be expressed in terms of an elliptic integral of the first kind. In fact, set

$$P(x) = \frac{1 - 1/x_0}{x_0^2} X(x)$$

with

$$X(x) = x \left( x^3 - \frac{x_0^2}{1 - 1/x_0} (x - 1) \right).$$

The zeros of the quartic  $X(x)$  are

$$r_1 = x_0, \quad r_2 = \frac{x_0}{2(-1 + x_0)} \left[ 1 - x_0 + \sqrt{-3 + 2x_0 + x_0^2} \right],$$

$$r_2 = \frac{x_0}{2(-1 + x_0)} \left[ 1 - x_0 - \sqrt{-3 + 2x_0 + x_0^2} \right], \quad r_4 = 0.$$

Note that  $r_1 > r_2 > r_3 > r_4$ . It can be shown (e.g., Hancock 1958, p. 47) that

$$\int_{x_0}^{\infty} \frac{dx}{\sqrt{X(x)}} = \frac{2}{(r_1 - r_3)(r_2 - r_4)} F(\phi, k), \quad (6)$$

where

$$F(\phi, k) = \int_0^\phi (1 - k \sin^2 \phi)^{-1/2} d\phi$$

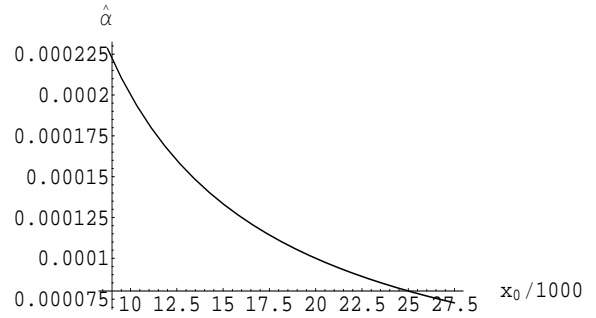
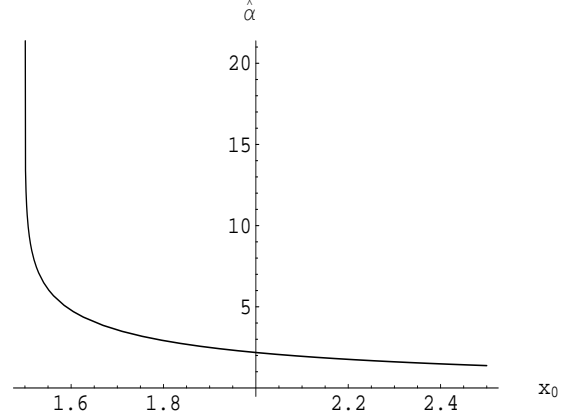


**Figure 1.** Bending angle  $\hat{\alpha}$  (in radians) as a function of  $x_0 = r_0/r_\bullet$ , where  $r_0$  is the distance of closest approach to the black hole. In the top graph, we see that  $\hat{\alpha}$  diverges as  $x_0 \rightarrow 3/2$ . The bottom graph shows that  $\hat{\alpha}$  is significantly less than unity for  $x_0 \gtrsim 8.75 \times 10^3$ . In the case of the Galactic black hole, the range of  $x_0$  in the bottom graph corresponds to a distance of closest approach in the interval  $2.29 \times 10^{-3} \text{ pc} \lesssim r_0 \lesssim 7.19 \times 10^{-3} \text{ pc}$ . This yields a lens-source distance ranging from about 10 pc to 100 pc — see Figure 2.

is an elliptic integral of the first kind with arguments

$$\phi = \sin^{-1} \sqrt{\frac{r_2 - r_4}{r_1 - r_4}}, \quad k = \frac{(r_1 - r_4)(r_2 - r_3)}{(r_1 - r_3)(r_2 - r_4)}.$$

Using (6), we plot the bending angle  $\hat{\alpha}$  in Figure 1. In addition, Taylor expanding the integrand of in (5) yields the following expansion for the bending angle (Virbhadra & Ellis 2000, Eiroa, Romero & Torres 2002):

$$\hat{\alpha}(x_0) = \frac{2}{x_0} + \left( \frac{15}{16}\pi - 1 \right) \frac{1}{x_0^2} + \mathcal{O}\left(\frac{1}{x_0^3}\right). \quad (7)$$

For light rays that travel directly from the source to the observe without looping around the black hole, assumption **A3** yields that  $1/x_0 \ll 1$ . By (7), the bending angle takes the standard weak-field form:

$$\hat{\alpha}(x_0) \approx \frac{2}{x_0}.$$

Because  $|\hat{\alpha}| \ll 1$  in this case and  $|\vartheta| \ll 1$  by (4), we obtain  $|\hat{\alpha} - \vartheta| \ll 1$  and, hence,

$$\tan(\hat{\alpha} - \vartheta) \approx \hat{\alpha} - \vartheta. \quad (8)$$

For the source-to-observer rays that do not loop, we have  $1/x_0 \approx r_\bullet/(\vartheta D_L)$ . Combined with equations (3), (4), and (8) we see that the lens equation reduces to the usual *weak-field lens equation*:

$$\beta = \vartheta - \frac{D_{LS}}{D_S} \hat{\alpha}(\vartheta) = \vartheta - \frac{\theta_E^2}{\vartheta}, \quad (9)$$

where

$$\theta_E = \sqrt{\frac{2D_{LS} r_\bullet}{D_L D_S}}. \quad (10)$$

For rays that loop around the black hole at least once before arriving at the observer, the bending angle  $\hat{\alpha}$  is near a multiple of  $2\pi$  (cf. Figure 1). Such light rays are close to the unstable photon orbit at radius  $3r_g$  (e.g., Chandrasekhar 1992, p. 132). In this case, the bending angle has the form  $\hat{\alpha} = 2n\pi + \Delta\hat{\alpha}_n$ , where  $n \geq 1$  is the number of times the light ray loops around the black hole and  $|\Delta\hat{\alpha}_n| \ll 1$  (representing a small angular deviation from a multiple of  $2\pi$ ). Consequently,

$$\tan(\alpha - \vartheta) \approx \Delta\alpha_n - \vartheta. \quad (11)$$

Equation (11), along with **A1** and **A2**, yields the following *strong-field lens equation* for rays circling near  $3r_g$  (Bozza et al. 2001):

$$\beta = \vartheta - \frac{D_{LS}}{D_S} \Delta\alpha_n. \quad (12)$$

We now turn to the solutions of the weak- and strong-field lens equations.

## 2.2 Einstein ring, Primary and Secondary Images

The solutions of the weak-field lens equation (9) are well known (e.g., see Petters, Levine & Wambsganss (2001), pp. 187-191, for a detailed treatment).

If  $\beta = 0$  (source is on the optical axis), then the source is lensed into a formally infinitely magnified circle, called an *Einstein ring*, which has an angular radius  $\theta_E$ .

If  $\beta \neq 0$  (source is off the optical axis), then on opposite sides of the black hole there are a primary image  $\vartheta_+^{\text{wf}}$  and secondary image  $\vartheta_-^{\text{wf}}$  of the source:

$$\vartheta_{\pm}^{\text{wf}} = \frac{\theta_E}{2} \left[ (\beta/\theta_E) \pm \sqrt{(\beta/\theta_E)^2 + 4} \right] \approx \pm\theta_E + \frac{\beta}{2}. \quad (13)$$

The primary and secondary images have magnification

$$\mu_{\pm}^{\text{wf}} = \frac{(\beta/\theta_E)^2 + 2}{2|\beta/\theta_E| \sqrt{(\beta/\theta_E)^2 + 4}} \pm \frac{1}{2} \approx \frac{\theta_E}{2|\beta|}. \quad (14)$$

Note that assumption **A1** was used for the approximations in (13) and (14). The total magnification is

$$\mu_{\text{wf}} = \mu_+^{\text{wf}} + \mu_-^{\text{wf}} = \frac{\theta_E}{|\beta|}.$$

To simplify expressions like (13) and (14) that involve  $\theta_E$ , we shall scale all angles as follows:

$$u = \frac{\beta}{\theta_E}, \quad \theta = \frac{\vartheta}{\theta_E},$$

The weak-field image positions and magnifications now become

$$\theta_{\pm}^{\text{wf}} = \frac{u}{2} \pm 1, \quad \mu_{\pm}^{\text{wf}} = \frac{1}{2|u|}, \quad \mu_{\text{wf}} = \frac{1}{|u|}. \quad (15)$$

Note that the angular image positions and magnifications in (15) for the weak field regime coincide with that obtained from lensing by a point mass.

## 2.3 Relativistic Einstein rings

If  $\beta = 0$ , then the source is lensed into the formally infinitely magnified Einstein ring mentioned in Section 2.2, along with an infinite sequence of relativistic Einstein rings near  $3r_g$ . The angular radii  $\vartheta_n^E$  of the relativistic Einstein rings are given by the solutions of the strong-field lens equation (12) for  $\beta = 0$  (Bozza et al. 2001):

$$\vartheta_n^E = \vartheta_\bullet (A_0 e^{-(2n+1)\pi} + B_0), \quad (16)$$

where

$$\vartheta_\bullet = \frac{r_\bullet}{D_L}, \quad A_0 = \sqrt{3} \left( \frac{18}{2 + \sqrt{3}} \right)^2, \quad B_0 = \frac{3\sqrt{3}}{2}.$$

Note that  $\vartheta_\bullet$  is approximately the angle spanned by the Schwarzschild radius. For simplicity, set

$$d_n^\bullet = A_0 \vartheta_\bullet e^{-(2n+1)\pi}$$

and rewrite  $\vartheta_n^E$  as

$$\vartheta_n^E = d_n^\bullet + \vartheta_\bullet B_0.$$

Since  $\vartheta_\bullet \ll 1$ , we have  $d_1^\bullet < 1$  (because  $A_0 e^{-3\pi} \approx 3.25 \times 10^{-3}$ ). Consequently, each term in the strictly decreasing sequence  $\{d_n^\bullet\}_{n=1}^\infty$  obeys

$$d_n^\bullet \leq d_1^\bullet < 1, \quad n = 1, 2, \dots \quad (17)$$

## 2.4 Relativistic Images

If  $\beta \neq 0$ , then we know from Section 2.2 that on opposite sides of the black hole there are a primary image  $\vartheta_+^{\text{wf}}$  and secondary image  $\vartheta_-^{\text{wf}}$  from light rays that travel directly (no looping around the black hole) to the observer. In addition, there are two infinite sequences (on opposite sides of the black hole) of relativistic images  $\vartheta_n^\pm$  that are due to light rays looping  $n$  times around the black hole near  $3r_g$ . The following expressions for the solutions  $\vartheta_n^\pm$  of the strong-field lens equation (12) are convenient (Bozza et al. 2001):

$$\vartheta_n^\pm = \pm\vartheta_n^E + \frac{D_S}{D_{LS}} d_n^\bullet \beta. \quad n = 1, 2, \dots \quad (18)$$

The images  $\vartheta_n^+$  (resp.,  $\vartheta_n^-$ ) result from  $n$  clockwise (resp., counter-clockwise) windings around the black hole.

Using (2), the magnifications of the relativistic images can be shown to be approximately as follows (Bozza et al. 2001, Eiroa, Romero & Torres 2002):

$$\mu_n^\pm = \frac{D_S}{D_{LS}} \vartheta_n^E d_n^\bullet \frac{1}{|\beta|}. \quad (19)$$

The total magnification is then

$$\mu_R = \sum_{n=1}^{\infty} \mu_n^+ + \sum_{n=1}^{\infty} \mu_n^-.$$

Equations (16) and (19) imply that

$$\mu_R = \frac{2 D_S}{|\beta| D_{LS}} \left[ \sum_{n=1}^{\infty} (d_n^\bullet)^2 + B_0 \vartheta_\bullet \sum_{n=1}^{\infty} d_n^\bullet \right]. \quad (20)$$

By (17), both series in (20) are geometric series. Hence,

$$\mu_R = \frac{2 D_S \vartheta_{\bullet}^2 C_0}{D_{LS} |\beta|}, \quad (21)$$

where

$$C_0 = A_0 \left[ A_0 \frac{e^{-6\pi}}{1 - e^{-4\pi}} + B_0 \frac{e^{-3\pi}}{1 - e^{-2\pi}} \right]. \quad (22)$$

Equations (18), (19), and (21) simplify to

$$\theta_n^{\pm} = \pm \theta_n^E + \frac{D_S}{D_{LS}} d_n^{\bullet} u, \quad \theta_n^E = \frac{\vartheta_n^E}{\theta_E}, \quad (23)$$

$$\mu_n^{\pm} = \frac{D_S}{D_{LS}} \theta_n^E d_n^{\bullet} \frac{1}{|u|}, \quad (24)$$

$$\mu_R = \frac{2 D_S \vartheta_{\bullet}^2 C_0}{D_{LS} \theta_E |u|}. \quad (25)$$

By (25), the relativistic and total magnifications for a point source are then given as follows (Bozza et al. 2001, Eiroa, Romero & Torres 2002):

$$\mu_R = C_R \mu_{\text{wf}}, \quad \mu_{\text{tot}} = \mu_{\text{wf}} + \mu_R = (1 + C_R) \mu_{\text{wf}}, \quad (26)$$

where

$$C_R = \frac{2 D_S \vartheta_{\bullet}^2 C_0}{D_{LS} \theta_E} = 4 C_0 \theta_{\bullet}^3, \quad \theta_{\bullet} = \frac{\vartheta_{\bullet}}{\theta_E}. \quad (27)$$

Equation (26) shows that  $C_R$  determines the relativistic correction to the total weak-field magnification.

We also refer interested readers to the elegant generalization by Eiroa, Romero & Torres (2002) of equations (23)–(25) to the case of a Reissner-Nordström black hole lens.

### 3 IMAGE CENTROID

In this section, we derive a formula using **A1–A3** that expresses the image centroid of a Schwarzschild black hole as a relativistic correction to the weak-field image centroid of a point mass lens.

#### 3.1 Image Centroid Formula

The center-of-light or centroid of all the images of a source at  $u$  is

$$\Theta_{\text{cent}} = \frac{(\mu_+ \theta_+ + \mu_- \theta_-) + \sum_{n=1}^{\infty} (\mu_n^+ \theta_n^+ + \mu_n^- \theta_n^-)}{\mu_{\text{tot}}}, \quad (28)$$

where  $\mu_{\text{tot}}$  is the total magnification. Since the centroid shift is

$$\delta \Theta_{\text{cent}} = \Theta_{\text{cent}} - u,$$

it suffices to study  $\Theta_{\text{cent}}$ .

We now express the image centroid as

$$\Theta_{\text{cent}} = \frac{\mu_{\text{wf}}}{\mu_{\text{tot}}} \Theta_{\text{cent}}^{\text{wf}} + \frac{\mu_R}{\mu_{\text{tot}}} \Theta_{\text{cent}}^{\text{R}}, \quad (29)$$

where  $\Theta_{\text{cent}}^{\text{wf}}$  and  $\Theta_{\text{cent}}^{\text{R}}$  are respectively the centroids of the weak-field and relativistic images. Explicitly,

$$\Theta_{\text{cent}}^{\text{wf}} = \frac{\mu_+^{\text{wf}} \theta_+^{\text{wf}} + \mu_-^{\text{wf}} \theta_-^{\text{wf}}}{\mu_{\text{wf}}}$$

and

$$\Theta_{\text{cent}}^{\text{R}} = \frac{\sum_{n=1}^{\infty} (\mu_n^+ \theta_n^+ + \mu_n^- \theta_n^-)}{\mu_R}.$$

By (15) and (25), the weak-field image centroid is

$$\Theta_{\text{cent}}^{\text{wf}} = \frac{u}{2}. \quad (30)$$

Recall that (30) is the weak-field image centroid for source positions near the caustic. Indeed, the full shifted image centroid due to a point mass lens is an ellipse (e.g., Høg, Novikov & Polnarev 1995, Miyamoto & Yoshi 1995, Walker 1995).

Using (23) and (24), we get

$$\Theta_{\text{cent}}^{\text{R}} = \frac{2}{\mu_R} \left( \frac{D_S}{D_{LS}} \right)^2 \frac{u}{|u|} \sum_{n=1}^{\infty} \theta_n^E (d_n^{\bullet})^2.$$

Now, observe that

$$\sum_{n=1}^{\infty} \theta_n^E (d_n^{\bullet})^k = \frac{C_0(k) \vartheta_{\bullet}^{k+1}}{\theta_E}, \quad k = 1, 2, \dots, \quad (31)$$

where

$$C_0(k) = A_0^k [A_0 E(k+1) + B_0 E(k)] \quad (32)$$

with

$$E(k) = \frac{e^{-3k\pi}}{1 - e^{-2k\pi}}.$$

Note that  $C_0(1) = C_0$ . Equation (31) yields

$$\Theta_{\text{cent}}^{\text{R}} = \frac{2}{\mu_R} \left( \frac{D_S}{D_{LS}} \right)^2 \frac{C_0(2) \vartheta_{\bullet}^3}{\theta_E} \frac{u}{|u|} = \frac{8 C_0(2) \theta_{\bullet}^5}{\mu_R} \frac{u}{|u|}.$$

Equations (26), (27), and (30) imply

$$\Theta_{\text{cent}}^{\text{R}} = D_R \Theta_{\text{cent}}^{\text{wf}}, \quad (33)$$

where

$$D_R = 4 \frac{C_0(2)}{C_0(1)} \theta_{\bullet}^2. \quad (34)$$

Hence, the image centroid (29) simplifies to

$$\Theta_{\text{cent}} = C_{\text{cent}} \Theta_{\text{cent}}^{\text{wf}}, \quad (35)$$

where

$$C_{\text{cent}} = \frac{1 + D_R C_R}{1 + C_R}. \quad (36)$$

It follows that the constants  $C_R$  and  $D_R$  determine the full relativistic correction to the image centroid due to a point mass lensing a source near the caustic.

#### 3.2 Extended Source

The total magnification of an extended source  $D$  with surface brightness  $S$  is given by

$$\mu_{\text{tot}}^{\text{ext}} = \frac{\int_D d\mathbf{u} S(\mathbf{u}) \mu_{\text{tot}}(\mathbf{u})}{\int_D d\mathbf{u} S(\mathbf{u})},$$

where  $\mathbf{u} = u \hat{\beta}$  with  $\hat{\beta} = \beta/|\beta|$ , the unit angular vector position of the source. The spherical symmetry of the Schwarzschild black hole implies that  $\mu_{\text{tot}}(\mathbf{u}) = \mu_{\text{tot}}(u)$ . Consequently, equation (26) yields

$$\mu_{\text{tot}}^{\text{ext}} = (1 + C_R) \mu_{\text{wf}}^{\text{ext}}, \quad (37)$$

where

$$\mu_{\text{wf}}^{\text{ext}} = \frac{\int_D d\mathbf{u} S(\mathbf{u}) \mu_{\text{wf}}(u)}{\int_D d\mathbf{u} S(\mathbf{u})}$$

is the weak-field extended source total magnification. Readers are referred to Witt & Mao (1994) for a discussion of  $\mu_{\text{wf}}^{\text{ext}}$  for a point mass lens.

The image centroid of the extended source is

$$\Theta_{\text{cent}}^{\text{ext}} = \frac{\int_D d\mathbf{u} S(\mathbf{u}) \Theta_{\text{cent}} \mu_{\text{tot}}(\mathbf{u})}{\int_D d\mathbf{u} S(\mathbf{u}) \mu_{\text{tot}}(\mathbf{u})}.$$

Equation (35) gives

$$\Theta_{\text{cent}}^{\text{ext}} = C_{\text{cent}} \Theta_{\text{cent}}^{\text{ext, wf}}, \quad (38)$$

where

$$\Theta_{\text{cent}}^{\text{ext, wf}} = \frac{\int_D d\mathbf{u} S(\mathbf{u}) \Theta_{\text{cent}}^{\text{wf}}(u) \mu_{\text{wf}}(u)}{\int_D d\mathbf{u} S(\mathbf{u}) \mu_{\text{wf}}(u)}$$

is the weak-field extended image centroid — see Mao & Witt (1998) for a treatment of  $\Theta_{\text{cent}}^{\text{ext, wf}}$  with a point mass lens. Thus, as in the point source case, the quantities  $C_{\text{R}}$  and  $D_{\text{R}}$  determine the relativistic corrections to the extended source image centroid, as well as the total magnification, for a point mass lens.

#### 4 APPLICATIONS TO THE GALACTIC BLACK HOLE LENS

In this section, we estimate the relativistic corrections to the weak-field total magnification and image centroid for the case of the Galactic black hole under **A1–A3**.

We begin with estimates of some needed quantities. The constants  $C_0(1)$  and  $C_0(2)$  are given approximately as follows:

$$C_0(1) \approx 8.47 \times 10^{-3}, \quad C_0(2) \approx 2.75 \times 10^{-5}.$$

For the massive black hole at the Galactic center, we have (Ghez et al. 1998):

$$M_{\bullet} \approx 2.6 \times 10^6 M_{\odot}, \quad D_L \approx 8.5 \text{ kpc}.$$

The linear and angular Schwarzschild radii of the black hole are

$$r_{\bullet} \approx 5.23 \times 10^{-2} \text{ AU}, \quad \vartheta_{\bullet} = \frac{r_{\bullet}}{D_L} \approx 6.46 \mu\text{as}. \quad (39)$$

Since the relativistic images are near  $3r_{\bullet}/2$ , those on opposite sides of the black hole have angular spacings of order  $3\vartheta_{\bullet} \approx 19.38 \mu\text{as}$ , which is outside the resolving capabilities of near-future instruments. The expected resolution of the Space Interferometry Mission to be launched in 2009 is about 10 mas. Hence, the source is microlensed by the strong-field region near the black hole.

The (weak-field) angular Einstein radius as a function of the lens-source distance  $x = D_{LS}$  is given by

$$\theta_{\text{E}}(x) = \left( \frac{2\vartheta_{\bullet} x}{D_L + x} \right)^{1/2} \approx 1.65 \sqrt{\frac{x}{D_L + x}} \text{ as}. \quad (40)$$

The function  $\theta_{\text{E}}(x)$  has a positive derivative and so is strictly increasing — see Figure 2. The angular diameter of the Einstein ring is approximately the angular spacing between the primary and secondary images. For  $10 \text{ pc} \leq x \leq 100 \text{ pc}$ , the

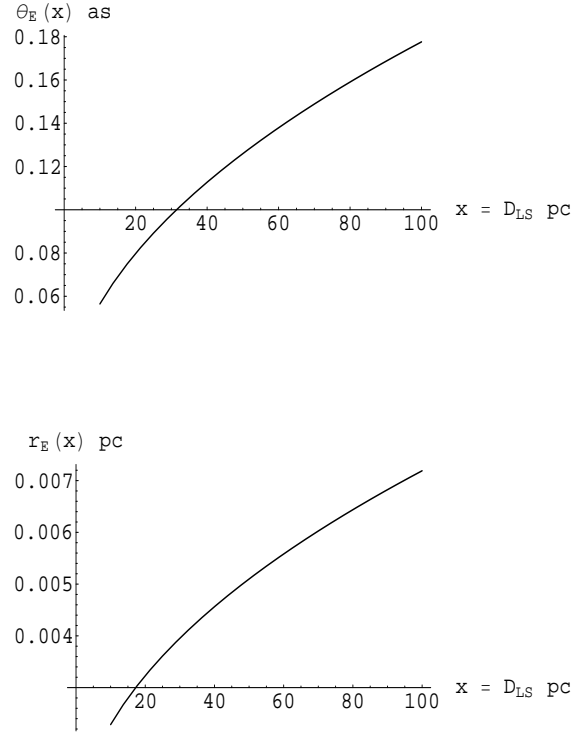


**Figure 2.** The angular (top graph) and linear (bottom graph) Einstein ring radii as a function of lens-source distance in the range  $10 \text{ pc} \leq D_{LS} \leq 100 \text{ pc}$ . For these distances, the linear Einstein ring radius  $r_{\text{E}}$  approximates the distance  $r_0$  of closest approach as well as the impact parameter  $b$  (since  $r_0 \approx b$ ). The value of  $r_{\text{E}}$  is approximately  $2.29 \times 10^{-3} \text{ pc}$  for  $D_{LS} \approx 10 \text{ pc}$ .

range of the angular spacing is  $0.1 \text{ as} \lesssim 2\theta_{\text{E}}(x) \lesssim 0.4 \text{ as}$ , which is at the boundary of the resolving capabilities of present day instruments.

We also have

$$\theta_{\bullet}(x) = \frac{\vartheta_{\bullet}}{\theta_{\text{E}}(x)} \approx 3.922 \times 10^{-6} \sqrt{\frac{D_L + x}{x}}$$

and by (34) we get

$$D_{\text{R}}(x) \approx 2 \times 10^{-13} \left( \frac{D_L + x}{x} \right). \quad (41)$$

Let us now verify that assumptions **A1–A3** hold. We are supposing that  $|\beta| \ll 1$  and  $D_{LS} \geq 10 \text{ pc}$ , which by (39) yields  $D_{LS}/r_{\bullet} \approx 3.82 \times 10^7 \gg 1$ , so assumption **A1** is satisfied. Now, the largest value  $b_{\text{max}}$  of the impact parameter of light rays from the source to the observer occurs for the rays that travel to the observer without looping around the black hole. These rays passing through the nearly flat region outside the black hole, which means that the associated impact parameter and distance of closest approach are approximately equal. Equation (13) shows that the angular positions of the closest approach of the light rays are given approximately by  $\pm\theta_{\text{E}}$  (since  $|\beta| \ll 1$ ). It follows that  $b_{\text{max}}$  can be approximated by the linear Einstein ring radius,  $r_{\text{E}}(x) = D_L \theta_{\text{E}}(x)$  (Figure 2). The function  $x/r_{\text{E}}(x)$  is

strictly increasing with a minimum value of approximately  $x/r_E(x) \gtrsim 4.38 \times 10^3 \gg 1$  for  $x \gtrsim 10$  pc — see Figure 3. In addition, since  $r_E(x)$  is also strictly increasing with maximum  $r_E^{\max} \approx 8 \times 10^{-6} D_L$  for  $x \gg D_L$  (see (40)), it follows that  $D_L/r_E \gtrsim D_L/r_E^{\max} \approx 1.3 \times 10^5 \gg 1$ . Consequently, assumption **A2** holds. Now, since  $r_\bullet/r_E(x)$  is strictly decreasing with a maximum value of order  $10^{-4}$  for  $x \gtrsim 10$  pc, the primary and secondary images lie in the nearly flat region outside the black hole. In particular, assumption **A3** is also satisfied.

We add that since  $r_\bullet/x$  is at most of order  $10^{-8}$  for  $x \gtrsim 10$  pc, a source at distance  $x$  lies in a region of space that is “flatter” than the region near the linear Einstein radius  $r_E(x)$  (since  $r_\bullet/r_E(x) \lesssim 10^{-4}$ ). Furthermore, for a source star of mass  $M_*$  and radius  $R_*$ , the closest it can get to the Galactic black hole without being torn apart is given roughly by the tidal disruption radius of the source (e.g., Magorrian & Tremaine 1999):

$$r_{\text{tidal}} \approx 137.5 \left( \frac{\eta_*^2 M_\bullet}{2.6 \times 10^6 M_\odot} \right)^{1/3} \left( \frac{M_\odot}{M_*} \right)^{1/3} R_*,$$

where  $\eta_*$  is a parameter of order unity that depends on the model of the source. For  $M_* \approx M_\odot$  and  $r_* \approx R_\odot$ , the tidal radius is then of order

$$r_{\text{tidal}} \approx 137.5 R_\odot \approx 0.64 \text{ AU}.$$

Hence, a source at  $x \gtrsim 10$  pc is significantly outside its tidal disruption radius.

For the Galactic black hole, equation (27) shows that the relativistic correction to the weak-field total magnification is

$$C_R(x) \approx 2.1 \times 10^{-18} \left( \frac{D_L + x}{x} \right)^{3/2}. \quad (42)$$

Since the derivative of  $C_R(x)$  is always negative, the correction  $C_R(x)$  is a strictly decreasing function of the lens-source distance  $x$  — see Figure 4. The figure shows that the relativistic correction  $C_R$  to the magnification is at most of order  $5 \times 10^{-14}$  for sources with  $D_{LS} \gtrsim 10$  pc.

Turning to the relativistic image centroid, equations (41) and (42) yield that the derivative of  $D_R(x)C_R(x)$  is always negative. Consequently, the function  $D_R(x)C_R(x)$  is strictly decreasing with increasing lens-source distance — Figure 4. Furthermore, the figure yields that  $C_R(x)$  is at most of order  $10^{-14}$  and  $D_R(x)C_R(x)$  at most of order  $10^{-24}$  for  $x \gtrsim 10$  pc, so the relativistic image centroid factor (36) can be approximated as follows:

$$C_{\text{cent}}(x) \approx 1 - C_R(x) \quad \text{for } x \gtrsim 10 \text{ pc}. \quad (43)$$

It follows that the relativistic correction  $C_R$  to the weak-field total magnification also serves as a relativistic correction to the weak-field image centroid. The value  $C_R(x) = 1$  corresponds to the weak-field case, which clearly holds approximately for  $x \gtrsim 10$  pc. In light of Figure 4, measurable relativistic corrections to the total magnification and image centroid due to standard gravitational lensing by the Galactic black hole would most likely require sources very close to the black hole.

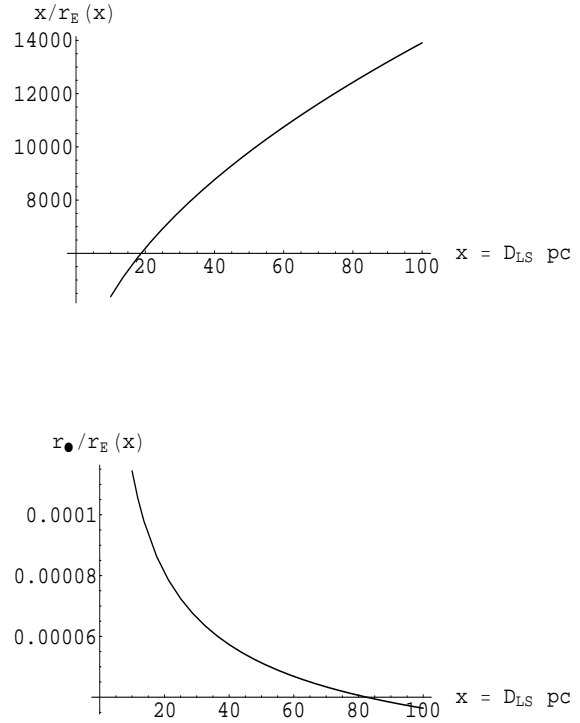


**Figure 3.** The top graph shows that  $D_{LS} \gg r_E$  for  $D_{LS} \gtrsim 10$  pc, while the bottom illustrates that  $r_\bullet/r_E \ll 1$ . The latter implies that the primary and secondary images lie in the nearly flat region outside the Galactic black hole.

## 5 CONCLUSION

Previous work on gravitational lensing by the black hole at the Galactic center investigated the relativistic corrections to the weak-field total magnification and image centroid to second order in  $1/x_0 = 2GM/(r_0c^2)$ , where  $r_0$  is the distance of closest approach of the light ray to the black hole. It was shown recently that for a point mass lens the total magnification and image centroid shift of a point source remain unchanged by relativistic corrections of second order in  $1/x_0$ . We computed the relativistic corrections for a Schwarzschild black hole lens under assumptions **A1–A3**. These corrections were applied to the case of the massive black hole at the Galactic center. We found that the weak-field magnification and image centroid have approximately the same relativistic correction. This correction is a strictly decreasing function of the lens-source distance  $D_{LS}$ . For  $D_{LS} \gtrsim 10$  pc, the relativistic correction is of order at most  $10^{-14}$ , a minuscule correction. Hence, for standard lensing configurations, a nontrivial relativistic correction to microlensing by the Galactic black hole would most likely have to come from sources deep inside the black hole’s potential well.

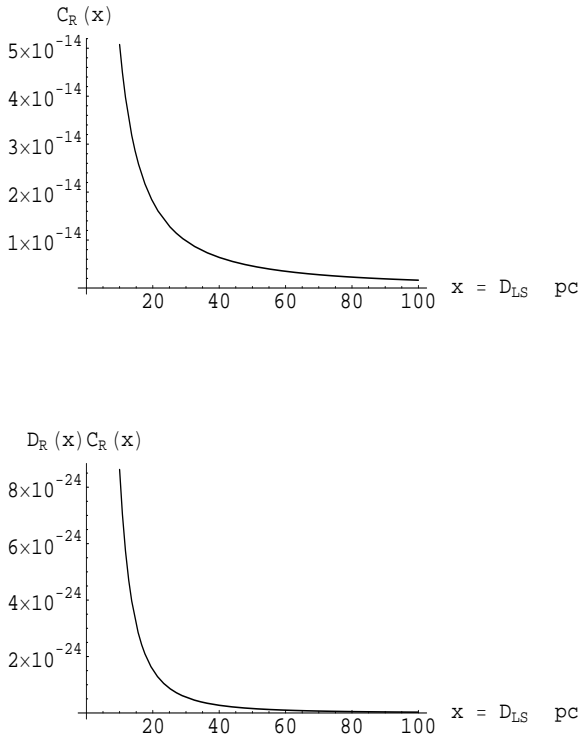


**Figure 4.** The quantities  $C_R$  and  $D_R C_R$  as a function of the distance  $D_{LS}$  of the source from the Galactic black hole, where  $10 \text{ pc} \leq D_{LS} \leq 100 \text{ pc}$ . Note that these distances are significantly outside the tidal disruption radius,  $r_{\text{tidal}} \approx 0.64 \text{ AU}$ , for a sun-like source. The bottom figure guarantees that  $C_R$  describes the relativistic correction to both the weak-field image centroid and total magnification (see discussion in text). The correction is clearly negligible for sources  $D_{LS} \gtrsim 10 \text{ pc}$ .

## ACKNOWLEDGMENTS

Many thanks to Scott Gaudi for stimulating discussions and the referee for a helpful clarifying comment. This work was supported in part by an Alfred P. Sloan Research Fellowship and NSF Career grant DMS-98-96274.

## REFERENCES

- Alexander, T., 2001, *ApJ.*, 553, L149  
 Alexander, T., Loeb, A., 2001, *ApJ.*, 551, 223  
 Alexander, T., Sternberg, A., 1999, *ApJ.*, 520, 137  
 Boden, A.F., Shao, M., & van Buren, D., 1998, *ApJ*, 502, 538  
 Bozza, V., Capozziello, S., Iovane, G., and Scarpetta, G., 2001, *Gen. Rel. Grav.*, 33, 1535  
 Chandrasekhar, S., 1992, *The Mathematical Theory of Black Holes*. Oxford University Press, Oxford  
 Ebina, J., Osuga, T., Asada, H., Kasai, M., 2000, *Prog. Theor. Phys.*, 104, 1317  
 Eiroa, E., Romero, G., Torres, D., 2002, *Phys. Rev. D*, 66, 024010.

- Fragile, P. C., Mathews, G. J., 2000, *ApJ.*, 542, 328  
 Frittelli, S., Kling, T., Newman, E. T., 2000, *Phys. Rev. D*, 61, 064021  
 Gaudi, B.S., Petters, A.O., 2002, *ApJ.*, 574. In press.  
 Ghez, A. M., Klein, B. L., Morris, M., Becklin, E. E., 1998, *ApJ.*, 509, 678  
 Hancock, H., 1958, *Elliptic Integrals*. Dover, New York  
 Høg, E., Novikov, I. D., Polnarev, A. G., 1995, *ApJ*, 294, 287.  
 Jaroszynski, M., 1998a, *Acta Astron.*, 48, 413  
 Jaroszynski, M., 1998b, *Acta Astron.*, 48, 653  
 Jaroszynski, M., 1999, *ApJ*, 521, 591  
 Jeong, Y., Han, C., Park, S., 1999, *ApJ.*, 511, 569  
 Lewis, G. F., Wang, X. R., 2001, *Prog. Theor. Phys.*, 105, 893  
 Magorrian, J., Tremaine, S., 1999, *Mon. Not. R. Astron. Soc.*, 309, 447  
 Mao, S., Witt, H., 1998, *Mon. Not. R. Astron. Soc.*, 300, 1041  
 Misner, C., Thorne, K., Wheeler, J., 1973, *Gravitation*. W. H. Freeman and Company, San Francisco  
 Miyamoto, M., Yoshi, Y., 1995, *Astron. J.*, 110, 1427.  
 Ohanian, H., 1987, *Am. J. Phys.*, 55, 428  
 Paczynski, B., 1996, *ARA&A*, 34, 419  
 Paczyński, B., 1998, *ApJ*, 494, L23  
 Petters, A.O., Levine, H., Wambsganss, J., 2001, *Singularity Theory and Gravitational Lensing*. Birkhäuser, Boston  
 Virbhadra, K.S., Ellis, G., 2000, *Phys. Rev. D.*, 62, 084003  
 Wald, R. M., 1984, *General Relativity*. The University of Chicago Press, Chicago  
 Walker, M. A., 1995, *ApJ*, 453, 37.  
 Wardle, M., Yusef-Zadeh, F., 1992, *ApJ.*, 387, L65  
 Weinberg, S., 1972, *Gravitation and Cosmology*. John Wiley & Sons, New York  
 Witt, H., Mao, S., 1994, *ApJ.*, 430, 505